# Integrated mRNA and miRNA transcriptome analysis provides novel insights into the molecular mechanisms underlying goose pituitary development during the embryo-to-hatchling transition

Qingyuan Ouyang,[1] Shenqiang Hu,[1,2] Li Li,[1] Mingxia Ran, Jiaran Zhu, Yiting Zhao, Bo Hu, Jiwei Hu, Hua He, Liang Li, and Jiwen Wang

*Farm Animal Genetic Resources Exploration and Innovation Key Laboratory of Sichuan Province, Sichuan Agricultural University, Chengdu, Sichuan, 611130, China*

**ABSTRACT** It is well established that the endocrine system plays a pivotal role in preparing the avian embryos for the abrupt switch from chorioallantoic to pulmonary respiration during the critical embryo-to-hatchling transition. However, as the master gland of the endocrine system, there has been little research focusing on the molecular mechanisms controlling the development and function of the pituitary gland during the peri-hatch period in birds. In the present study, we aimed to determine the genome-wide mRNA and miRNA transcriptome profiles of the pituitary during the embryo-to-hatchling transition period from embryonic day 22 (**E22**) to post-hatching day 6 (**P6**) in the goose (*Anser cygnoides*). Of note, expression of *Anser_cygnoides_newGene_32456* and *LOC106031011* were significantly different among these 4 stages (i.e., E22, E26, P2, and P6). Meanwhile, the neuroactive ligand-receptor interaction pathway was significantly enriched by the DEGs commonly identified among three pairwise comparisons. At the miRNA transcriptome level, there were not commonly identified DE miRNAs among these 4 stages, while the 418 of their predicted target genes were mutually shared. Both the target genes of DE miRNAs in each comparison and these 418 shared target genes were significantly enriched in the ECM-receptor interaction and focal adhesion pathways. In the predicted miRNA-mRNA interaction networks of these 2 pathways, novel_miRNA_467, novel_miRNA_154, and novel_miRNA_340 were the hub miRNAs. In addition, multiple DE miRNAs also showed predicted target relationships with the DEGs associated with extracellular matrix (**ECM**) components. Among them, expression of novel_miR_120, tgu-miR-92-3p, and novel_miR_398 was significantly negatively correlated with that of *LAMC3* (laminin subunit gamma3), suggesting that these miRNAs may regulate pituitary tissue remodeling and functional changes through targeting *LAMC3* during development. These identified DE mRNAs and miRNAs as well as their predicted interaction networks involved in regulation of tissue remodeling and cellular functions were most likely to play critical roles in facilitating the embryo-to-hatchling transition. These results provide novel insights into the early developmental process of avian pituitary gland and will help better understand the underlying molecular mechanisms.

**Key words:** goose, pituitary, embryo-to-hatchling transition, mRNA, miRNA

## INTRODUCTION

Pituitary is known as the master gland of the endocrine system in vertebrates and plays essential roles in a wide spectrum of biological activities such as growth and development, immune and metabolism, and reproduction (Musumeci et al., 2015). Anatomically, the vertebrate pituitary is comprised of multiple cell types, including corticotrophs, somatotrophs, lactotrophs, gonadotrophs, thytrophs, melanocyte stimulating hormone (**MSH**) secretory cells, and folliculo-stallate (**FS**) cells (Le Tissier et al., 2012). The orderly differentiation and functional maturation of these cell components are undoubtedly a prerequisite for ensuring the versatile functions of the pituitary (Ooi et al., 2004). Of note, it has been previously reported that both the anatomical structures and developmental dynamics of the pituitary gland vary significantly between mammals and birds

(Scanes, 2015), especially during embryonic and early post-hatching life (Scanes et al., 2005). Since the embryo's responses to new environmental challenges may have short- and long-term impacts on the physiology and performance, it is therefore of particular interest to dissect the molecular mechanisms regulating the development and function of the avian pituitary during the peri-hatch period, eventually helping better understand how the embryo adapts itself to the abrupt environmental changes during the critical embryo-to-hatchling transition.

In order to adapt well to the sudden environmental changes during the embryo-to-hatchling transition, both the morphology and functions of liver, thyroid, and ovary have changed simultaneously during this period in birds (McNabb, 2006; Cogburn et al., 2018; Hu et al., 2020). As the critical regulator of the development and functions of these tissues or organs, there is evidence that the pituitary histomorphology and gene expression profiles also change remarkably during early developmental stage. Moreover, species-specific differences in gene expression profiles during early pituitary development have been previously shown in domestic birds. In the chicken pituitary, the mRNA expression levels of growth hormone (**GH)** and prolactin (**PRL)** started to increase on embryonic day 16 (**E16**) and E18, respectively (Kansaku et al., 1994), while those of duck *GH* and *IGF1* started to increase on E25 and E21, respectively (Hu et al., 2015). Although the chicken pituitary transcriptome changes in the post-hatching development have been previously investigated (Pritchett et al., 2017; Ellestad et al., 2019), there are still lack of studies on the avian pituitary developmental dynamics during the critical embryo-to-hatchling transition, especially in waterfowls.

In recent years, high-throughput sequencing technologies have been demonstrated to be efficient and reliable to study the developmental dynamics of the avian muscle and ovarian tissues during the embryonic to early post-hatching stages (Liu et al., 2019). In the meantime, as a class of non-coding RNAs, miRNAs have also been shown to be involved in regulating the growth, development, and metabolism of multiple avian tissues (Fu et al., 2018; Li et al., 2019). Therefore, the objectives of this study were to: 1) explore the dynamic changes in the goose pituitary mRNA and miRNA transcriptomes during the peri-hatch period and 2) identify the key mRNAs, miRNAs as well as the miRNA-mRNA interaction networks involved in facilitating the embryo-to-hatchling transition. These data will provide new insights into the molecular mechanisms underlying early pituitary development in birds.

## MATERIALS AND METHODS

### Ethics Statement

All geese were obtained from the Waterfowl Breeding Experimental Farm of Sichuan Agricultural University. All experimental procedures that involved in animal manipulation were approved by the Institutional Animal Care and Use Committee (**IACUC**) of Sichuan Agricultural University (Chengdu Campus, Sichuan, China) under Approval No. 20180034.

### Sample Collection and RNA Extraction

Four representative developmental stages during goose embryo-to-hatchling transition, including **E22**, **E26**, post-hatching day 2 (**P2**), and **P6**, were selected for sample collection. Six female geese with similar weights at each developmental stage were randomly selected from 150 geese hatched from the same batch and euthanized by carbon dioxide anesthesia and exsanguination by severing the carotid artery, and the pituitary gland from each individual was snap-frozen into liquid nitrogen and finally stored at −80℃ until RNA isolation. According to the manufacturer's protocol, the total RNA was extracted from all collected samples using the miRNeasy Mini Kit (Qiagen, Hilden, Germany). The extraction, purity, concentration, and integrity of RNA were determined by Nanodrop (Thermo Fisher Scientific, Wilmington, DE) and Agilent Bioanalyzer 2100 (Agilent Technologies, Santa Clara, CA). The criteria used to select the RNA for following analysis were A260/A280≥1.8, A260/A230≥2.0 and RNA integrity number >7.0.

### Library Construction and Sequencing

To satisfy the requirements for sequencing, 2 hypophyses were pooled for each replicate on E22, E26, P2, and P6 (Supplementary Table S4). Twelve mixed RNA samples were used for library construction. Total RNA was used to prepare a small RNA (**sRNA**) library according to instructions of NEBNext Multiplex sRNA Library Prep Set for Illumina (Illumina, San Diego, CA). The sRNA library was validated by using an Agilent Bioanalyzer 2100 system (Agilent Technologies, Santa Clara, CA) to check its size and purity. The NEBNext Poly (A) mRNA magnetic separation module (NEB, E7490, Ipswich, MA) was used to isolate mRNA. The cDNA library was constructed using the NEBNext Ultra RNA Library Prep Kit from Illumina (NEB, E7530, Ipswich, MA) and the NEB Multiplex Oligos from Illumina (NEB, E7500, Ipswich, MA) as per the manufacturer's instructions. All libraries were sequenced using Illumina HiSeq 2500 (Illumina, San Diego, CA). The original sequencing data for this study can be found in the Sequence Read Archive (https://www.ncbi.nlm.nih.gov/sra) at NCBI, with the BioProject ID: PRJNA649062.

### Bioinformatic Analysis

Raw data of RNA-seq were processed using the NGS QC Toolkit (version 2.3.3) (Patel and Jain, 2012). Reads that contained poly-N and low-quality reads were removed to obtain clean reads. Clean reads were mapped to the goose reference genome (https://www.ncbi.nlm.

nih.gov/assembly/GCF_000971095.1/) using the HISAT2 software (version 2.1.0) (Daehwan et al., 2015). StringTie (version 1.3.3b) (Mihaela et al., 2015) was used to assemble transcripts after integrating all individual transcripts and genes.

Raw data in fastq format were firstly processed using in-house perl scripts. Clean data were obtained by removing reads that contain adapters, ploy-N, and low-quality reads. Reads were trimmed and cleaned by removing the sequences smaller than 18nt or longer than 30nt. Bowtie software (version 1.2.3) was used for sequence alignment of clean reads and Silva databases, GtRNAdb databases, Rfam databases, and Repbase databases. The remaining reads were used to detect known miRNA and novel miRNA predicted by comparing with Genome. The potential target genes of miRNAs were predicted using miRanda (Betel et al., 2008) and targetscan (Lewis et al., 2003) softwares.

Differential expression analysis among groups was performed using the R package EBseq (version 1.29.0) (Leng et al., 2013). The P values were adjusted using the Benjamini and Hochberg's approach in order to control the false discovery rate. The RNAs and miRNAs with an adjusted P-value (FDR) <0.05 and |Fold change| >1.5 analyzed by EBseq were regarded as DE mRNAs and miRNAs. Gene ontology enrichment analysis software tools (**GOEAST**) (Zeng and Wang, 2008) was used to analyze the Gene Ontology (**GO**) functions. KOBAS3.0 (Ai and Kong, 2018) was used to analyze the Kyoto Encyclopedia of Genes and Genomes (**KEGG**) functions.

Cytoscape software (version 3.7.2) (Shannon et al., 2003) was used to show the targeting relationship between DE miRNAs and their target genes. String online software (Szklarczyk et al., 2019) was used to display protein interaction networks between target genes.

## Quantitative Real-Time PCR Analysis

Total RNA extracted from each pituitary was reverse transcribed into cDNA using a Revert Aid First Strand cDNA Synthesis Kit (Thermo, MA). Primer 5.0 was used to design the primers for quantitative real-time PCR (**qRT-PCR**) (Table 1). The PCR reactions were performed on the CFX96TM Real-Time PCR Detection System (BioRad, Hercules, CA) using the SYBR Premix Ex TaqTM II (Takara Biotechnology Co., Ltd., Dalian, China). Each sample was repeated in 3 times. The relative expression levels of the target genes in the samples were normalized to the reference genes $GAPDH$ and $\beta$-$ACTIN$ using the comparative Cq method ($\Delta\Delta$Cq) (Schmittgen and Livak, 2008).

## Statistical Analysis

The expression levels of DEG were expressed as the mean ± SEM. Pearson's correlation coefficient was calculated to analyze the correlations between the expression of $LAMC3$ and several miRNAs (novel_miR_120, tgu-miR-92-3p, and novel_miR_398). Duncan's

**Table 1.** Primers used for qRT-PCR in this study.

| Primer name | Sequence (5'-3') | Product length (bp) |
|---|---|---|
| $PRL$-F | ACCTCCTTGCCTATCTGCCC | 162 |
| $PRL$-R | TGTAATGAAACCCCGACCCT | |
| $TSHR$-F | CCGTCAGCCTTCTGCGAGT | 164 |
| $TSHR$-R | GAGATGTTGGGGAGATTGGA | |
| $MCHR2$-F | ATCTCAGAAGAAAACTATCCCAG | 149 |
| $MCHR2$-R | AGGTTATGATGGTACAAAGAAGG | |
| $COL4A4$-F | ATGCCAGCCGAAATGATAAGT | 103 |
| $COL4A4$-R | GCACATCTGCTTATGTAGGGTTGTA | |
| $COL4A6$-F | CAATGAAGTGTGCTACTACGC | 233 |
| $COL4A6$-R | TGTGCATGAGGAAGGAGTATC | |
| $COL4A5$-F | GAAGGGTTATGTGAGCAGGG | 124 |
| $COL4A5$-R | TTCCGGTTCCTATACAATTGAA | |
| $FSH\beta$-F | GTGGTGCTCAGGATACTGCTTCA | 209 |
| $FSH\beta$-R | GTGCAGTTCAGTGCTATCAGTGTCA | |
| $LAMC3$-F | TGGGAAACTCCTTGTCTGTCT | 172 |
| $LAMC3$-R | GTGAACTCCTGCTGGGTCTTG | |
| $TSH\beta$-F | GCATCACTTTGTGCTCCTTCAGA | 122 |
| $TSH\beta$-R | TTGCCATTGCTGTCCCGAGT | |
| $THBS4$-F | ATACACAGGAGACCAAGTTAGG | 186 |
| $THBS4$-R | GGGTAGCCATCAATGTCAAC | |
| $THBS2$-F | GAGTGGGCTGTTGTGGCTTG | 174 |
| $THBS2$-R | CGGTATGCTGGGATAGTGGG | |
| $COL2A1$-F | CCTGGACGCCATCAAGGTTTT | 168 |
| $COL2A1$-R | TCGCCGTAGCTGAAGTGGAAG | |
| $LOC106031011$-F | CAGAAGCCTTATCTCAGTGGT | 95 |
| $LOC106031011$-R | CAAACAGTGTCCTTGAAAACG | |
| $VWF$-F | GTGGGCTATGCGGAAACTACA | 245 |
| $VWF$-R | AATGGGACTGACTTCACGGTG | |
| $COL6A6$-F | GTGGTCTATAGCTCTACGCCG | 188 |
| $COL6AA6$-R | GTGACAGCAAGTGACGATGGA | |
| $GAPDH$-F | GCTGATGCTCCCATGTTCGTGAT | 86 |
| $GAPDH$-R | GTGGTGCAAGAGGCATTGCTGAC | |
| $\beta$-$ACTIN$-F | CAACGAGCGGTTCAGGTGT | 92 |
| $\beta$-$ACTIN$-R | TGGAGTTGAAGGTGGTCTCGT | |

multiple range test was used to compare the differences in the expression levels of *LAMC3,* novel_miR_120, tgu-miR-92-3p, and novel_miR_398 at E22, E26, P2, and P6. *P*-value <0.05 was considered statistically significant. All statistical analyses were carried out using the SPSS 27.0 software.

## RESULTS

### Overview of the mRNA Transcriptome of Goose Pituitary During the Peri-hatch Period

A total of 99.57 Gb clean bases were obtained from 12 samples through mRNA sequencing, and 75.69% ~ 80.84% of the sequencing reads were aligned to the goose reference genome (Supplementary Table S1). As shown in Supplementary Figures 1A and 1B, 3 biological replications at each sampling point were well clustered together. Moreover, three biological replications on E22 were closer to those on E26, so were those on P2 and on P6. There were 303, 880, and 118 DEGs identified between E22_vs._E26, E26_vs._P2, and P2_vs._P6, respectively (Figure 1A). Meanwhile, 74, 33, and 11 DEGs were overlapped in E22_vs._E26 and E26_vs._P2, E26_vs._P2 and P2_vs._P6, and E22_vs._E26 and P2_vs._P6, respectively (Figure 1B). As shown in Figure 1B, there were 2 genes (i.e., *Anser_cygnoides_newGene_32456* and *LOC106031011*) whose expression in each sampling point was significantly different.

### Functional Enrichment Analysis of DEGs Between Goose Pituitaries at Different Developmental Stages

The top 20 KEGG pathways enriched by DEGs in 3 pairwise comparisons were shown in Figures 2A-2C. Of them, the AGE-RAGE signaling in diabetic complications, apelin signaling, adrenergic signaling in cardiomyocytes, and ECM-receptor interaction pathways were commonly enriched by the DEGs in E22_vs._E26 and E26_vs._P2. The focal adhesion and MAPK signaling pathways were commonly enriched by the DEGs in P2_vs._P6 and E26_vs._P2. However, the calcium signaling, phagosome, cytokine-cytokine receptor interaction, folate biosynthesis, mucin type O-glycan biosynthesis, cell cycle, vascular smooth muscle contraction, progesterone-mediated oocyte maturation, and gap junction pathways were only significantly enriched by the DEGs in E26_vs._P2.

As shown in Figure 2D, the neuroactive ligand-receptor interaction pathway was commonly significantly enriched by the DEGs in each pairwise comparisons. However, the expression profiles of these DEGs enriched in this pathway were different, as shown in Figure 2E. Besides, some DEGs related to hormone synthesis and secretion was also significantly enriched in the neuroactive ligand-receptor interaction pathway, and their expression in geese pituitaries at four developmental stages were also verified by qRT-PCR. As shown in Figure 2F, expression of almost all these selected DEGs displayed changes in the same direction with those observed using RNA-seq, indicating the true reliability of our Illumina sequencing methods. Expression of melanin-concentrating hormone receptor-2 (*MCHR2*) gradually increased during the peri-hatch period. Levels of prolactin (*PRL*) mRNA increased from E22 to P2 but underwent a decline on P6. Expression of follicle stimulating hormone β (*FSHβ*), thyroid stimulating hormone (*TSHβ*), and thyroid stimulating hormone receptor (*TSHR*) genes decreased from E22 to P2 until an increased on P6.

### Overview of the miRNA Transcriptome of Goose Pituitary During the Peri-hatch Period

As shown in Supplementary Table S2, 66.88% ~ 74.73% of the miRNA sequencing reads were aligned to
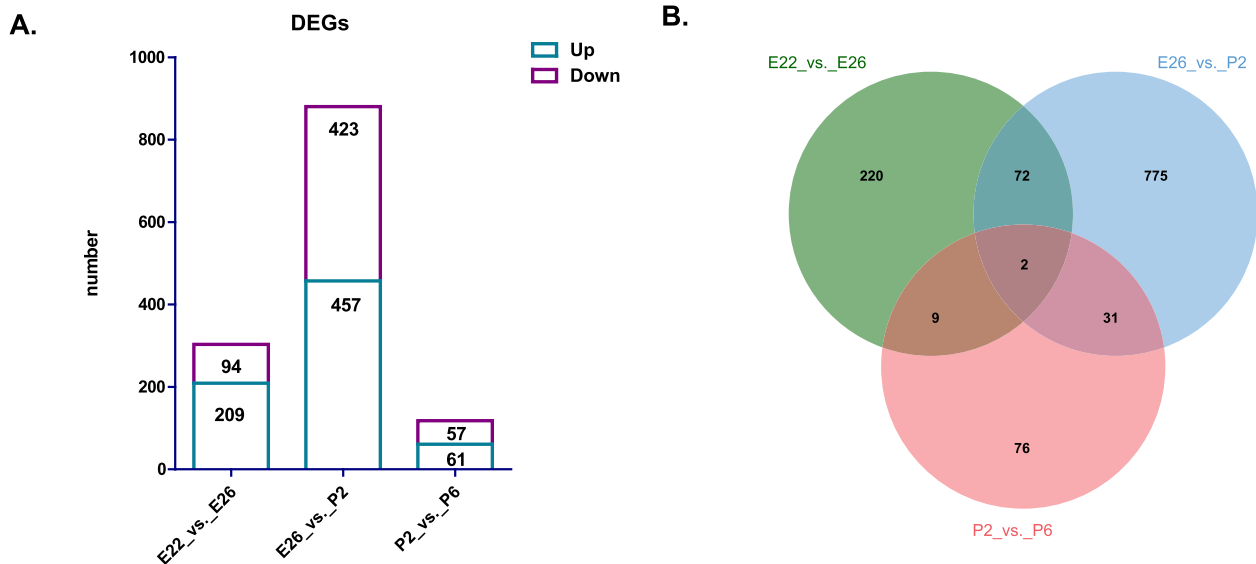


**Figure 1.** Genome-wide transcriptome changes in goose pituitaries at different developmental stages. (A) Histogram of the number of up- and downregulated genes among three pairwise comparisons. (B) Venn diagram of the common DEGs between three pairwise comparisons.
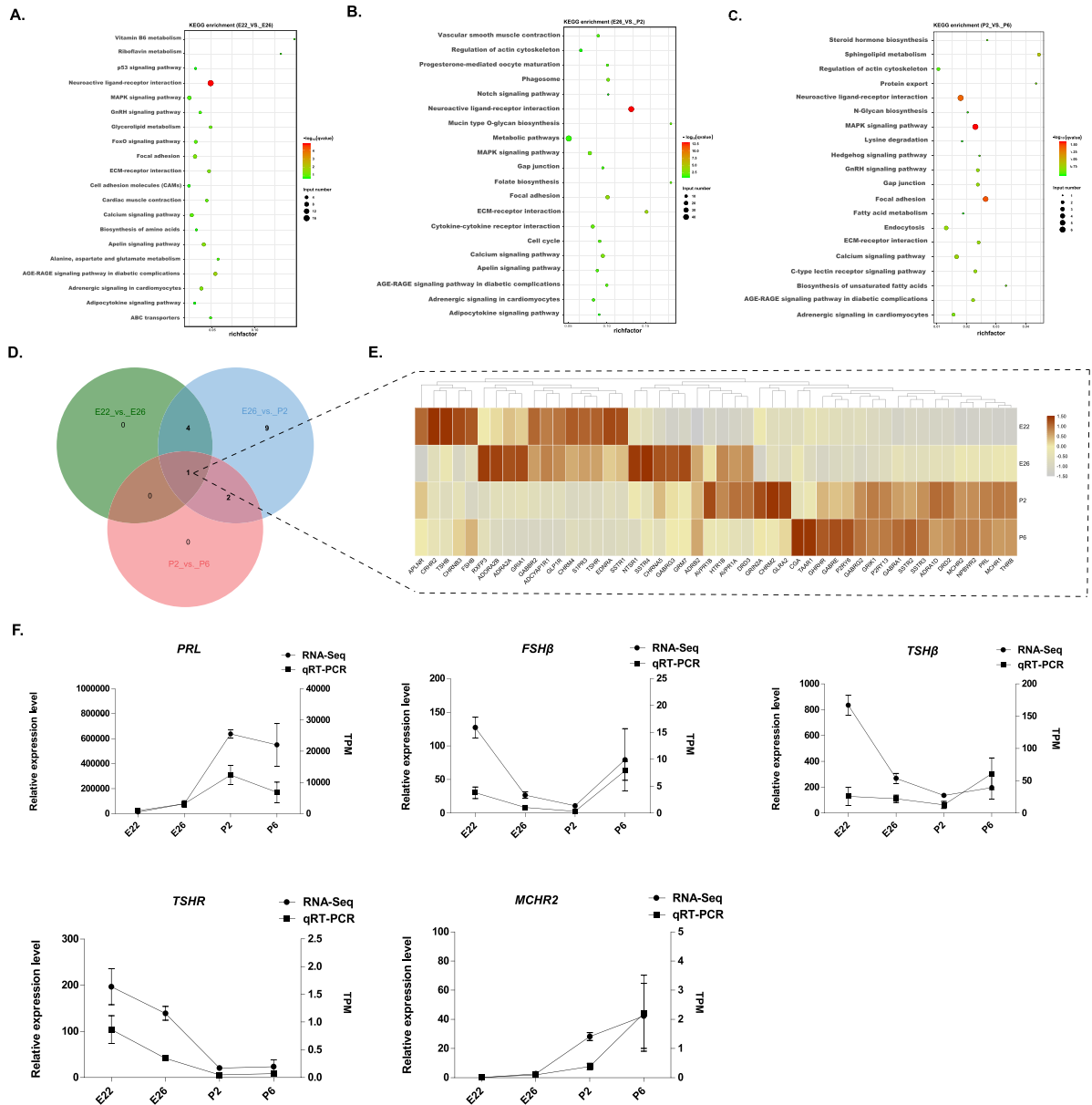
**Figure 2.** Functional annotation and qRT-PCR validation of the DEGs between geese pituitaries at different developmental stages. Top20 KEGG pathways enriched by the DEGs between E22_vs._E26 (A), E26_vs._P2 (B), and P2_vs._P6 (C), respectively. (D) Venn diagram of the common KEGG pathways significantly enriched by the DEGs in each pairwise comparison. (E) Heatmap analysis of the expression profiles of the DEGs in the neuroactive ligand-receptor interaction pathway during early goose pituitary development. (F) some DEGs in the neuroactive ligand-receptor interaction pathway. The results of qRT-PCR and RNA-Seq were expressed as the mean ±SEM (n = 3, three biological replications at each developmental stage). Abbreviations: KEGG, Kyoto Encyclopedia of Genes and Genomes; qRT-PCR, quantitative real-time PCR.

the goose reference genome. A total of 1,882 miRNAs were obtained from all samples, including 1,268 known-miRNAs and 614 novel-miRNAs. The length of known-miRNAs and novel-miRNAs were mainly distributed between 20 and 24nt, of which the miRNAs with a length of 22nt length were the most (Figure 3A). The first base at the 5'end of the known and novel miRNAs were shown to have a strong bias toward 'U' (Figure 3B). There were 78, 244, and 21 DE miRNAs identified between E22_vs._E26, E26_vs._P2, and P2_vs._P6, respectively. The E22_vs._E26 and P2_vs._P6 groups shared more than 50% of the DE miRNAs with the E26_vs._P2 group (Figure 3C). By predicting the target genes for these DE miRNAs, 1,302,

3,030, and 2,037 target genes were found in groups E22_vs._E26, E26_vs._P2, and P2_vs._P6, respectively, and 418 target genes were overlapped in three groups (Figure 3D).

## Integrated Analysis of Differentially Expressed mRNAs and miRNAs Between Goose Pituitaries at Different Developmental Stages

These 418 shared predicted target genes of DE miR-NAs in three pairwise comparisons were significantly enriched in the ECM-receptor interaction, focal
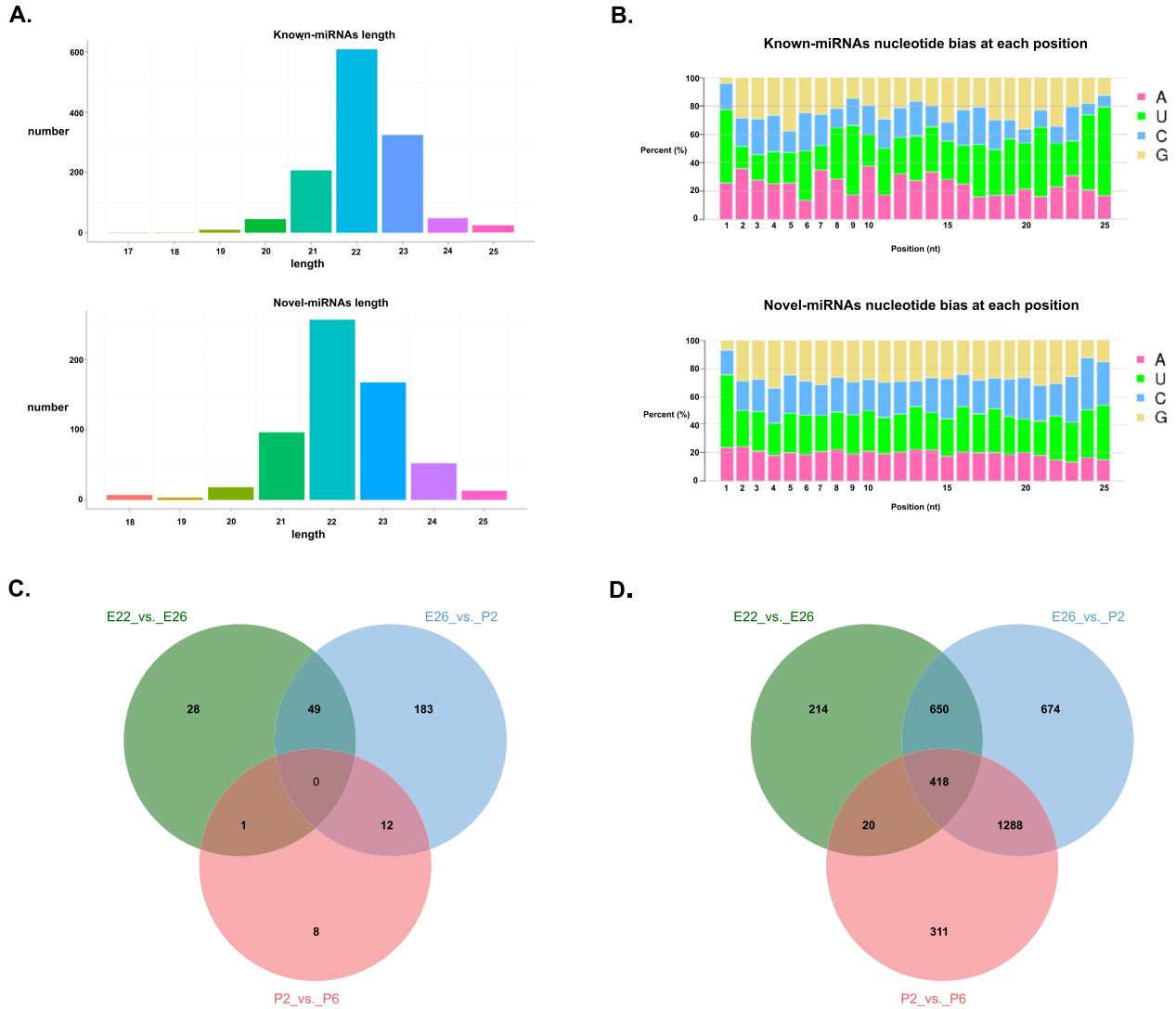
**Figue 3.** The characteristics and the number of DE miRNAs and their predicted target genes in three pairwise comparisons. (A) Histogram of the length of known and novel miRNAs. (B) Statistics of the first base preference of known and novel miRNAs. (C) Venn diagram of the common DE miRNAs between three pairwise comparisons. (D) Venn diagram of the target genes of DE miRNAs between three pairwise comparisons.

adhesion, and phosphatidylinositol signaling pathways (Supplementary Table S3). As shown in Figures 4A-4C, both the ECM-receptor interaction and focal adhesion pathways were commonly significantly enriched by the predicted target genes of DE miRNAs in each pairwise comparison. Furthermore, the interaction networks between 19 DE miRNAs and their 75 predicted target genes involved in the ECM-receptor interaction and focal adhesion pathways were constructed (Figure 4D). Of them, three miRNAs including novel_miRNA_467, novel_miRNA_154, and novel_miRNA_340 had the most number of target genes, which might be hub miR-NAs. Moreover, the correlation between expression of DE miRNAs and differentially expressed target genes were also analyzed. Among them, expression of three miRNAs including novel_miR_120, tgu-miR-92-3p, and novel_miR_398 showed significant negative corre-lations with that of *LAMC3* (Figure 4E, Supplementary Figure 2). In view of the central role of the ECM-recep-tor interaction pathway, we further verified the expres-sion levels of the collagen and laminin gene family

(*COL2A1, COL4A4, COL4A5, COL4A6, COL6A6*, and *LAMC3*) as well as 3 other DEGs (*THBS2, THBS4, and VWF*) involved in the ECM-receptor interaction path-way. As shown in Figure 4F, expression of almost all these selected DEGs determined by qRT-PCR showed changes in the same direction as those observed using RNA-Seq, further demonstrating the true reliability of the Illumina sequencing method. In addition, it should be noted that the expression profiles of the collagen gene family members were different. Among them, expression of *COL6A6* increased from E26 to P2 but the others gradually decreased during the peri-hatch period.

## DISCUSSION

Results from both PCA and heatmap analysis sug-gested that the pituitary transcriptome expression pro-files were much more similar between E22 and E26 (during the embryonic period) as well as between P2 and P6 (during the post-hatch period). Meanwhile, it
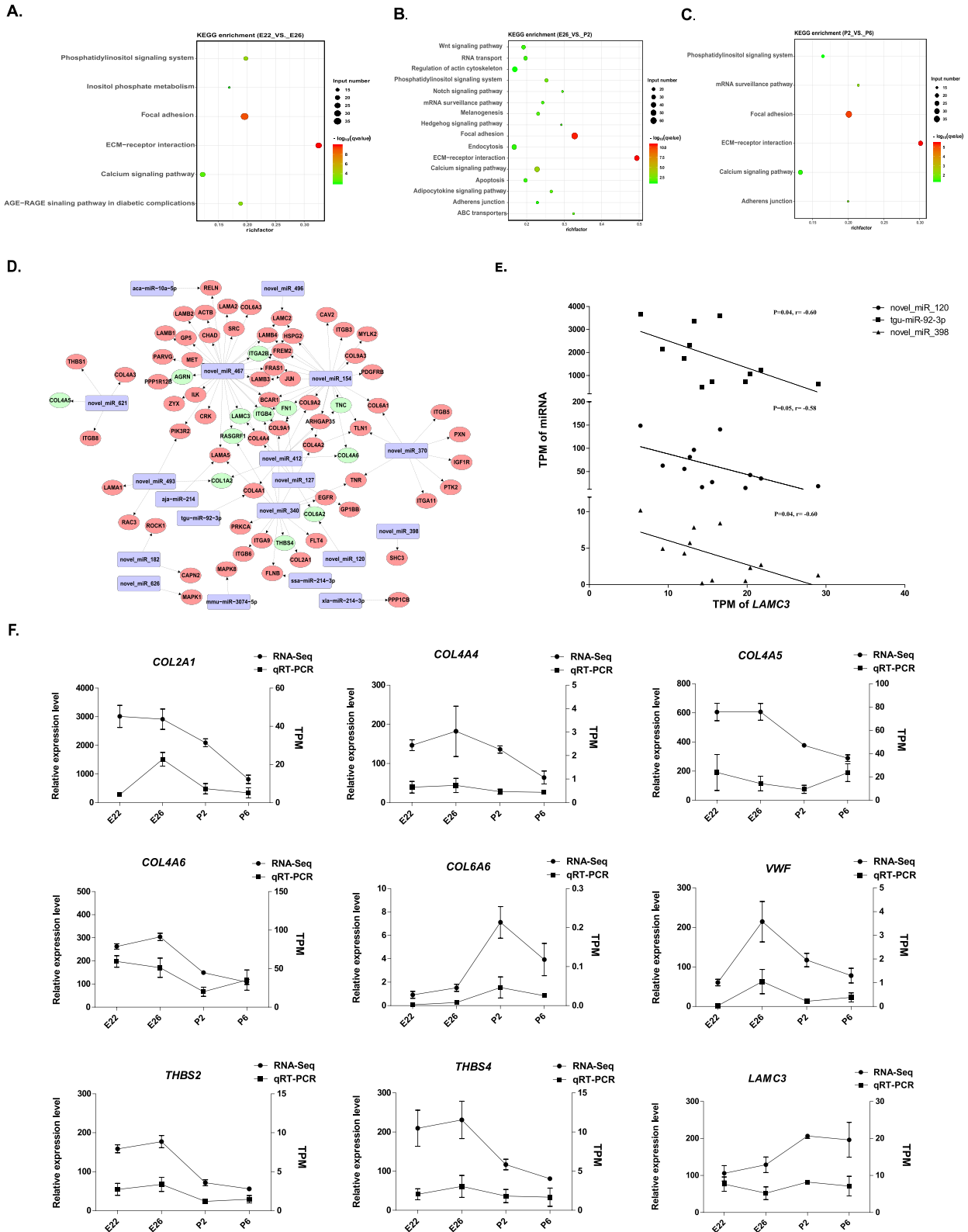
**Figure 4.** Functional analysis and qRT-PCR validation of the DE miRNAs and their target genes in pairwise comparisons. KEGG pathways significantly enriched by the predicted target genes of DE miRNAs between E22_vs._E26 (A), E26_vs._P2 (B), and P2_vs._P6 (C), respectively. (D) Interaction network analysis of DE miRNAs and their predicted target genes in relation to focal adhesion and ECM-receptor interaction pathways. (E) A scatter plot and trend line of expression of novel_miR_120, tgu-miR-92-3p, novel_miR_398, and *LAMC3*. (F) qRT-PCR validation of expression of the main DEGs involving the ECM-receptor interaction pathway. The results of qRT-PCR and RNA-Seq were expressed as the mean ±SEM (n = 3, three biological replications at each developmental stage). Abbreviations: ECM, xtracellular matrix; KEGG, Kyoto Encyclopedia of Genes and Genomes; qRT-PCR, quantitative real-time PCR.

was also observed that the number of both DEGs and DE miRNAs were the largest in E26_vs._P2 among 3 pairwise comparisons. These results altogether suggested that the goose pituitary transcriptome changes remarkably throughout the peri-hatch period, especially during the critical embryo-to-hatchling transition. Of note, 2 DEGs commonly present among 3 pairwise comparisons (*Anser_cygnoides_newGene_32456* and *LOC106031011*) were differentially expressed throughout the peri-hatch period. As a newly identified gene, there currently lacks understanding of the functions of *Anser_cygnoides_newGene_32456*. *LOC106031011* that encodes the cystine/glutamate transporter-like protein can catalyze the transport of L-glutamic acid coupled with $Na^+$ and $K^+$. Different types of glutamate receptors were shown to be present on the gland cells of the anterior pituitary (Petrusz, 1994; Villalobos et al., 1996). The latest studies found that glutamate mediated the apoptosis of prolactin-secreting cells and growth hormone-producing cells by activating type II metabotropic glutamate receptors (Pampillo et al., 2002; Caruso et al., 2004). Therefore, *LOC106031011* could be considered as one of the candidate genes regulating early goose pituitary development.

Based on the functional enrichment analysis of the DEGs in pairwise comparisons, it was proposed that the goose pituitary may help the individual adapt to sudden environmental changes during the peri-hatch period possibly by shaping its morphology and physiological functions, because the mostly-enriched pathways were related to tissue remodeling and regulation of cellular functions. Specifically, both the AGE-RAGE signaling and apelin signaling pathways were involved in vascular remodeling (Liu et al., 2016; Luo et al., 2018; Mughal and O'Rourke, 2018), but genes in these 2 pathways differ only in E22_vs._E26 and E26_vs._P2 group. It was shown that AGE and its interactions with RAGE induced vascular hypertrophy by promoting the accumulation of ECM and stimulating the proliferation while inhibiting the apoptosis of vascular smooth muscle cells (Prasad, 2019). The versatile functions of the pituitary also depend on the coordinated development of the vascular networks (Scully et al., 2016). In addition, platelets play a key role in regulating of angiogenesis (Walsh et al., 2015). As the genes related to platelet reaction, including *VWF, THBS2,* and *THBS4,* their expression levels vary drastically from E22 to P2, while be stable between P2 and P6, which indicated that the development of goose pituitary blood vessels was before P2. Importantly, the function of goose pituitary seems to be drastically changed from E26 to P2. The embryonic to hatchling transition is marked by changes in the nutrient supply from yolk during the embryonic stage to feed after hatching, which is undoubtedly accompanied by the metabolic function changes, such as altered folate biosynthesis and mucin type O-glycan biosynthesis (Jing et al., 2013). Of note, the specific enrichment of the DEGs identified between E26 and P2 in the progesterone-mediated oocyte maturation pathway indicated that

the maturation of goose oocytes could be closely related to developmental changes in the pituitary during this period. Previous studies have shown that the thickness of ovarian cortex and the volume of the oocytes increase after hatching (Hu et al., 2020). These results altogether indicated that the remodeling of the goose pituitary may take place before P2, and its functional changes were particularly dramatic during the embryo-to-hatchling transition.

In contrast to the KEGG pathways specifically enriched by the DEGs between different developmental stages, the neuroactive ligand-receptor interaction pathway was commonly significantly enriched by the DEGs in each pairwise comparison. Neuroactive substances are known to play a broad role in almost all physiology and organ development (Nässel and Zandawala, 2019). These DEGs in pairwise comparisons were involved in different categories of neuroactive substances, including rhodopsin like amine, peptide, hormone protein, nucleotide like, secretin like, and metabotropic glutamate/pheromone. As the largest class of neuroactive substances, peptide hormone can affect the growth and development or reproduction of animals in a wide range of physiological activities (van den Pol, 2012; Nusbaum et al., 2017). In particular, most of genes related to hormone synthesis and secretion involved in the neuroactive ligand-receptor interaction pathway were differentially expressed in the goose pituitary during different developmental stages, including *PRL, FSHβ, TSHβ, TSHR,* and *MCHR2*. In poultry, *PRL* is generally accepted as the crucial regulator of the onset and maintenance of broodiness (Wilkanowska et al., 2014). Previous studies showed that a progressive expression of *PRL* in the pituitary occurs 1-2 days before hatching (Ishida et al., 1991). Meanwhile, the increase in circulating PRL concentration has been suggested to cause ovarian regression and broodiness (Porter et al., 1991; Jiang et al., 2005; Edens, 2011). These results suggested that changes in expression of *PRL* may be associated with physiological changes during the embryo-to-hatchling transition. In addition to *PRL*, expression of *FSHβ, TSHβ, TSHR,* and *MCHR2* also varied in the goose pituitary during the peri-hatch period. Since the development of goose ovarian primary and secondary follicles begins after hatching (Hu et al., 2020), increased expression of *FSHβ* in the pituitary from P2 to P6 indicated that FSH synthesis and secretion by the pituitary could be essential for early goose ovarian follicle development. Previous studies have shown that thyroid hormone is required for growth and development of poultry (King and May, 1984). Thyroid hormone may be the most important hormones in establishing a state of metabolic readiness to promote the occurrence of thermoregulatory responses in the early postnatal period (McNabb et al., 1984). However, the expression levels of *TSHβ* and its receptor *TSHR* in different pituitary development stage were significantly different, and the expression trends of *TSHβ* and *TSHR* during the peri-hatch period were similar. These data indicated that thyroid hormone may act on the

pituitary gland through negative feedback after acting on other target tissues during the embryonic to post-hatching period. Although *MCH* has not been annotated in the genome of goose (Lu et al., 2015), their receptor (*MCHR2*) has been detected to be differentially expressed during the peri-hatch period. *MCHR2* is considered to be a functionally redundant pseudogene in chickens (Cui et al., 2017), its differential expression during the peri-hatch period seems to indicate its function in goose pituitary development. These results indicated that the function of the pituitary has undergone significant changes during early developmental stages, which are strongly associated with differential expression of genes involved in the neuroactive ligand-receptor interaction as well as hormone synthesis and secretion pathways.

Both the target genes of DE miRNAs and the 418 common target genes in pairwise comparisons were significantly enriched in the ECM-receptor interaction pathway. Previous reports have shown that ECM proteins are important for the normal morphology development in the pituitary (Paez-Pereda et al., 2005). ECM components can affect the function of FS cells and play an important role in guiding local cell arrangement in the anterior pituitary (Horiguchi et al., 2010). The individual components of the ECM, such as laminin, fibronectin and collagen, have effects on cell proliferation, differentiation, morphogenesis, and hormone production (Lukashev and Werb, 1998). Expression of multiple collagen gene family members, including *COL2A1, COL4A4, COL4A5, COL4A6,* and *COL6A6*, was significantly during different during the peri-hatch period. As a component of ECM, laminin maintains tissue structure and transmits biological information for cells (Aumailley and Gayraud, 1998). In this study, expression of *LAMC3* and *LAMA4* (laminin subunit alpha 4) were significantly different during the embryo-to-hatchling transition, but their expression profiles were opposite. Previous studies have shown that *LAMC3* is important for the development of the human brain (Barak et al., 2011), but there is no research on the role of *LAMA4* in the brain or pituitary development. Therefore, whether *LAMA4* can compensate for the function of *LAMC3* in the goose pituitary after hatching remains to be further studied. It is known that miRNAs usually inhibit the expression of their target genes. *LAMC3* has a significant negative correlation with the expression of novel_miR_120, tgu-miR-92-3p, and novel_miR_398, which has a predicted targeting relationship. At the same time, the expression of novel_miR_120, tgu-miR-92-3p, and novel_miR_398 were relatively high in miRNAs, these results indicated that novel_miR_120, tgu-miR-92-3p, and novel_miR_398 may be play a key role in goose pituitary development by targeting *LAMC3*. These results suggested that these identified DE miRNAs regulate the pituitary remodeling and functions possibly by targeting genes involved in the ECM-receptor interaction pathway.

In conclusion, this study represented the first to systematically describe the mRNA and miRNA transcriptome profiles in goose pituitary development during the peri-hatch period. These identified DE mRNAs and miRNAs as well as their predicted interaction networks involved in regulation of tissue remodeling and cellular functions were most likely to play critical roles in facilitating the embryo-to-hatchling transition. These results provide novel insights into the early developmental process of avian pituitary and will help better understand the underlying molecular mechanisms.

## ACKNOWLEDGMENTS

## DISCLOSURES

The authors have no conflicts of interest to report.

## SUPPLEMENTARY MATERIALS

Supplementary material associated with this article can be found in the online version at doi:10.1016/j. psj.2021.101380.

## REFERENCES

Ai, C., and L. Kong. 2018. CGPS: a machine learning-based approach integrating multiple gene set analysis tools for better prioritization of biologically relevant pathways. Genetics 45:489–504.

Aumailley, M., and B. Gayraud. 1998. Structure and biological activity of the extracellular matrix. J. Mol. Med. 76:253–265.

Barak, T., K. Y. Kwan, A. Louvi, V. Demirbilek, S. Saygı, B. Tüysüz, M. Choi, H. Boyacı, K. Doerschner, Y. Zhu, H. Kaymakçalan, S. Yılmaz, M. Bakırcıoğlu, A. O. Cağlayan, A. K. Oztürk, K. Yasuno, W. J. Brunken, E. Atalar, C. Yalçınkaya, A. Dinçer, R. A. Bronen, S. Mane, T. Ozçelik, R. P. Lifton, N. Sestan, K. Bilgüvar, and M. Günel. 2011. Recessive LAMC3 mutations cause malformations of occipital cortical development. Nat. Genet. 43:590–594.

Betel, D., M. Wilson, A. Gabow, D. S. Marks, and C. Sander. 2008. The microRNA.org resource: targets and expression. Nucleic Acids Res. 36:D149–D153.

Caruso, C., M. C. Bottino, M. Pampillo, D. Pisera, G. Jaita, B. Duvilanski, A. Seilicovich, and M. Lasaga. 2004. Glutamate induces apoptosis in anterior pituitary cells through group II metabotropic glutamate receptor activation. Endocrinology 145:4677–4684.

Cogburn, L. A., N. Trakooljul, C. Chen, H. Huang, C. H. Wu, W. Carré, X. Wang, and H. B. White 3rd. 2018. Transcriptional profiling of liver during the critical embryo-to-hatchling transition period in the chicken (Gallus gallus). BMC Genomics 19:695.

Cui, L., C. Lv, J. Zhang, C. Mo, D. Lin, J. Li, and Y. Wang. 2017. Characterization of melanin-concentrating hormone (MCH) and its receptor in chickens: tissue expression, functional analysis, and fasting-induced up-regulation of hypothalamic MCH expression. Gene 615:57–67.

Daehwan, K., L. Ben, and S. L. Salzberg. 2015. HISAT: a fast spliced aligner with low memory requirements. Nat. Methods 12:357–360.

Edens, F. W. 2011. Gender, age and reproductive status effects on serum prolactin concentrations in different varieties and species of poultry. Int. J. Poult. Sci. 10:832–838.

Ellestad, L. E., L. A. Cogburn, J. Simon, E. Le Bihan-Duval, S. E. Aggrey, M. S. Byerly, M. J. Duclos, and T. E. Porter. 2019. Transcriptional profiling and pathway analysis reveal differences in pituitary gland function, morphology, and vascularization in chickens genetically selected for high or low body weight. BMC Genomics 20:316.

Fu, S., Y. Zhao, Y. Li, G. Li, Y. Chen, Z. Li, G. Sun, H. Li, X. Kang, and F. Yan. 2018. Characterization of miRNA transcriptome profiles related to breast muscle development and intramuscular fat deposition in chickens. J. Cell. Biochem. 119:7063–7079.

Horiguchi, K., M. Kikuchi, K. Kusumoto, K. Fujiwara, T. Kouki, K. Kawanishi, and T. Yashiro. 2010. Living-cell imaging of transgenic rat anterior pituitary cells in primary culture reveals novel characteristics of folliculo-stellate cells. J. Endocrinol. 204:115–123.

Hu, S., S. Yang, Y. Lu, Y. Deng, L. Li, J. Zhu, Y. Zhang, B. Hu, J. Hu, L. Xia, H. He, C. Han, H. Liu, B. Kang, L. Li, and J. Wang. 2020. Dynamics of the transcriptome and accessible chromatin landscapes during early goose ovarian development. Front. Cell Dev. Biol. 8:196.

Hu, Y., H. Liu, C. Song, W. Xu, G. Ji, C. Zhu, J. Shu, and H. Li. 2015. Profiles of mRNA expression of related genes in the duck hypothalamus-pituitary growth axis during embryonic and early post-hatch development. Gene 559:38–43.

Ishida, H., K. Shimada, K. Sato, H. Seo, Y. Murata, N. Matsui, and D. Zadworny. 1991. Developmental expression of the prolactin gene in the chicken. Gen. Comp. Endocrinol. 83:463–467.

Jiang, R. S., G. Y. Xu, X. Q. Zhang, and N. Yang. 2005. Association of polymorphisms for prolactin and prolactin receptor genes with broody traits in chickens. Poult. Sci. 84:839–845.

Jing, M., G. B. Tactacan, and J. D. House. 2013. Post-hatching ontogeny of intestinal proton-coupled folate transporter and reduced folate carrier in broiler chickens. Anim. Int. J. Anim. Biosci. 7:1659–1664.

Kansaku, N., K. Shimada, O. Terada, and N. Saito. 1994. Prolactin, growth hormone, and luteinizing hormone-beta subunit gene expression in the cephalic and caudal lobes of the anterior pituitary gland during embryogenesis and different reproductive stages in the chicken. Gen. Comp. Endocrinol. 96:197–205.

King, D. B., and J. D. May. 1984. Thyroidal influence on body growth. J. Exp. Zool. 232:453–460.

Le Tissier, P. R., D. J. Hodson, C. Lafont, P. Fontanaud, M. Schaeffer, and P. Mollard. 2012. Anterior pituitary cell networks. Front. Neuroendocrinol. 33:252–266.

Leng, N., J. A. Dawson, J. A. Thomson, V. Ruotti, A. I. Rissman, B. M. Smits, J. D. Haag, M. N. Gould, R. M. Stewart, and C. Kendziorski. 2013. EBSeq: an empirical Bayes hierarchical model for inference in RNA-seq experiments. Bioinformatics 29:1035–1043.

Lewis, B. P., I. H. Shih, M. W. Jones-Rhoades, D. P. Bartel, and C. B. Burge. 2003. Prediction of mammalian microRNA targets. Cell 115:787–798.

Li, Q., S. Hu, Y. Wang, Y. Deng, S. Yang, J. Hu, L. Li, and J. Wang. 2019. mRNA and miRNA transcriptome profiling of granulosa and theca layers from geese ovarian follicles reveals the crucial pathways and interaction networks for regulation of follicle selection. Front. Genet. 10:988.

Liu, J., Q. Lei, F. Li, Y. Zhou, J. Gao, W. Liu, H. Han, and D. Cao. 2019. Dynamic transcriptomic analysis of breast muscle development from the embryonic to post-hatching periods in chickens. Front. Genet. 10:1308.

Liu, Y., M. Yu, L. Zhang, Q. Cao, Y. Song, Y. Liu, and J. Gong. 2016. Soluble receptor for advanced glycation end products mitigates vascular dysfunction in spontaneously hypertensive rats. Mol. Cell. Biochem. 419:165–176.

Lu, L., Y. Chen, Z. Wang, X. Li, W. Chen, Z. Tao, J. Shen, Y. Tian, D. Wang, G. Li, L. Chen, F. Chen, D. Fang, L. Yu, Y. Sun, Y. Ma, J. Li, and J. Wang. 2015. The goose genome sequence leads to insights into the evolution of waterfowl and susceptibility to fatty liver. Genome Biol. 16:89.

Lukashev, M. E., and Z. Werb. 1998. ECM signalling: orchestrating cell behaviour and misbehaviour. Trends Cell Biol. 8:437–441.

Luo, X., J. Liu, H. Zhou, and L. Chen. 2018. Apelin/APJ system: a critical regulator of vascular smooth muscle cell. J. Cell. Physiol. 233:5180–5188.

McNabb, F. M. 2006. Avian thyroid development and adaptive plasticity. Gen. Comp. Endocrinol. 147:93–101.

McNabb, F. M., F. W. Stanton, and S. G. Dicken. 1984. Post-hatching thyroid development and body growth in precocial vs altricial birds. Comp. Biochem. Physiol. A 78:629–635.

Mihaela, P., G. M. Pertea, C. M. Antonescu, C. Tsung-Cheng, J. T. Mendell, and S. L. Salzberg. 2015. StringTie enables improved reconstruction of a transcriptome from RNA-seq reads. Nat. Biotechnol. 33:290–295.

Mughal, A., and S. T. O'Rourke. 2018. Vascular effects of apelin: mechanisms and therapeutic potential. Pharmacol. Ther. 190:139–147.

Musumeci, G., S. Castorina, P. Castrogiovanni, C. Loreto, R. Leonardi, F. C. Aiello, G. Magro, and R. Imbesi. 2015. A journey through the pituitary gland: development, structure and function, with emphasis on embryo-foetal and later development. Acta Histochem. 117:355–366.

Nässel, D. R., and M. Zandawala. 2019. Recent advances in neuropeptide signaling in Drosophila, from genes to physiology and behavior. Prog. Neurobiol. 179:101607.

Nusbaum, M. P., D. M. Blitz, and E. Marder. 2017. Functional consequences of neuropeptide and small-molecule co-transmission. Nat. Rev. Neurosci. 18:389–403.

Ooi, G. T., N. Tawadros, and R. M. Escalona. 2004. Pituitary cell lines and their endocrine applications. Mol. Cell. Endocrinol. 228:1–21.

Paez-Pereda, M., F. Kuchenbauer, E. Arzt, and G. K. Stalla. 2005. Regulation of pituitary hormones and cell proliferation by components of the extracellular matrix. Braz. J Med. Biol. Res. 38:1487–1494.

Pampillo, M., S. Theas, B. Duvilanski, A. Seilicovich, and M. Lasaga. 2002. Effect of ionotropic and metabotropic glutamate agonists and D-aspartate on prolactin release from anterior pituitary cells. Exp. Clin. Endocrinol. Diab. 110:138–144.

Patel, R. K., and M. Jain. 2012. NGS QC Toolkit: a toolkit for quality control of next generation sequencing data. PLoS One 7:e30619.

Petrusz, P. 1994. The glutamate receptor subunit GLuR1 is expressed in gonadotrophs of the anterior pituitary and is regulated by gonadal feedback. Acta Biol. Hung. 45:387–397.

Porter, T. E., J. L. Silsby, B. M. Hargis, S. C. Fehrer, and M. E. el Halawani. 1991. Ovarian steroid production in vitro during gonadal regression in the turkey. II. Changes induced by forced molting. Biol. Reprod. 45:587–591.

Prasad, K. 2019. AGE-RAGE stress in the pathophysiology of pulmonary hypertension and its treatment. Int. J. Angiol. 28:71–79.

Pritchett, E. M., S. J. Lamont, and C. J. Schmidt. 2017. Transcriptomic changes throughout post-hatch development in Gallus gallus pituitary. J. Mol. Endocrinol. 58:43–55.

Scanes, C. G. 2015. Chapter 23 - Pituitary gland. Pages 497-533 in Sturkie's Avian Physiology. C. G. Scanes ed. 6th ed. Academic Press 92101, San Diego, CA.

Scanes, C. G., S. Jeftinija, A. Glavaski-Joksimovic, J. Proudman, C. Arámburo, and L. L. Anderson. 2005. The anterior pituitary gland: lessons from livestock. Domest. Anim. Endocrinol. 29:23–33.

Schmittgen, T. D., and K. J. Livak. 2008. Analyzing real-time PCR data by the comparative C(T) method. Nat. Protoc. 3:1101–1108.

Scully, K. M., D. Skowronska-Krawczyk, M. Krawczyk, D. Merkurjev, H. Taylor, A. Livolsi, J. Tollkuhn, R. V. Stan, and M. G. Rosenfeld. 2016. Epithelial cell integrin $\beta 1$ is required for developmental angiogenesis in the pituitary gland. Proc. Natl. Acad. Sci. U S A 113:13408–13413.

Shannon, P., A. Markiel, O. Ozier, N. S. Baliga, J. T. Wang, D. Ramage, N. Amin, B. Schwikowski, and T. Ideker. 2003. Cytoscape: a software environment for integrated models of biomolecular interaction networks. Genome Res. 13:2498.

Szklarczyk, D., A. G., D Lyon, A Junge, S Wyder, J Huerta-Cepas, M Simonovic, NT Doncheva, JH Morris, P Bork, LJ Jensen, and CV Mering. 2019. STRING v11: protein-protein association networks with increased coverage, supporting functional discovery in genome-wide experimental datasets. Nucleic Acids Res. 47:D607–D613.

van den Pol, A. N. 2012. Neuropeptide transmission in brain circuits. Neuron 76:98–115.

Villalobos, C., L. Núñez, and J. Garcia-Sancho. 1996. Functional glutamate receptors in a subpopulation of anterior pituitary cells. FASEB J. 10:654–660.

Walsh, T. G., P. Metharom, and M. C. Berndt. 2015. The functional role of platelets in the regulation of angiogenesis. Platelets 26: 199–211.

Wilkanowska, A., A. Mazurowski, S. Mroczkowski, and D. Kokoszyński. 2014. Prolactin (PRL) and prolactin receptor (PRLR) genes and their role in poultry production traits. Folia Biol. (Krakow) 62:1–8.

Zeng, Q., and X. J. Wang. 2008. GOEAST: a web-based software toolkit for Gene Ontology enrichment analysis. Nucleic Acids Res. 36(Web Server issue):W358–363, doi:10.1093/nar/gkn276. Epub 2008. May 16. PMID: 18487275; PMCID: PMC2447756.